


Gag-like proteins: Novel mediators of prenatal alcohol exposure in neural development

Marisa R. Pinson¹  | Dae D. Chung¹ | Amanda H. Mahnke^{1,2} | Nihal A. Salem¹ | Daniel Osorio³ | Vijay Nair¹ | Elizabeth A. Payne¹ | Jonathan J. del Real¹ | James J. Cai^{3,4,5,6} | Rajesh C. Miranda^{1,2,5} 

¹Department of Neuroscience and Experimental Therapeutics, Texas A&M University Health Science Center, Bryan, Texas, USA

²Women's Health in Neuroscience Program, Texas A&M University Health Science Center, Bryan, Texas, USA

³Department of Veterinary Integrative Biosciences, Texas A&M University, College Station, Texas, USA

⁴Department of Electrical and Computer Engineering, Texas A&M University, College Station, Texas, USA

⁵Interdisciplinary Program of Genetics, Texas A&M University, College Station, Texas, USA

⁶Center for Statistical Bioinformatics, Texas A&M University, College Station, Texas, USA

Correspondence

Rajesh C. Miranda, Department of Neuroscience and Experimental Therapeutics, Texas A&M University Health Science Center, College of Medicine, Medical Research and Education Building, 8447 Riverside Parkway, Bryan, TX 77807-3260, USA. Email: rmiranda@tamu.edu

Funding information

National Institute on Alcohol Abuse and Alcoholism, Grant/Award Number: F30 AA027698, F31 AA028446, R01 AA024659 and F99 NS113423

Abstract

Background: We previously showed that ethanol did not kill fetal neural stem cells (NSCs), but that their numbers nevertheless are decreased due to aberrant maturation and loss of self-renewal. To identify mechanisms that mediate this loss of NSCs, we focused on a family of Gag-like proteins (GLPs), derived from retroviral gene remnants within mammalian genomes. GLPs are important for fetal development, though their role in brain development is virtually unexplored. Moreover, GLPs may be transferred between cells in extracellular vesicles (EVs) and thereby transfer environmental adaptations between cells. We hypothesized that GLPs may mediate some effects of ethanol in NSCs.

Methods: Sex-segregated male and female fetal murine cortical NSCs, cultured *ex vivo* as nonadherent neurospheres, were exposed to a dose range of ethanol and to mitogen-withdrawal-induced differentiation. We used siRNAs to assess the effects of NSC-expressed GLP knockdown on growth, survival, and maturation and *in silico* GLP knockout, in an *in vivo* single-cell RNA-sequencing dataset, to identify GLP-mediated developmental pathways that were also ethanol-sensitive.

Results: PEG10 isoform-1, isoform-2, and PNMA2 were identified as dominant GLP species in both NSCs and their EVs. Ethanol-exposed NSCs exhibited significantly elevated PEG10 isoform-2 and PNMA2 protein during differentiation. Both PEG10 and PNMA2 were mediated apoptosis resistance and additionally, PEG10 promoted neuronal and astrocyte lineage maturation. Neither GLP influenced metabolism nor cell cycle in NSCs. Virtual PEG10 and PNMA2 knockout identified gene transcription regulation and ubiquitin-ligation processes as candidate mediators of GLP-linked prenatal alcohol effects.

Conclusions: Collectively, GLPs present in NSCs and their EVs may confer apoptosis resistance within the NSC niche and contribute to the abnormal maturation induced by ethanol.

KEYWORDS

extracellular vesicles, gag-like proteins, neural stem cells, prenatal alcohol exposure

This is an open access article under the terms of the Creative Commons Attribution-NoDerivs License, which permits use and distribution in any medium, provided the original work is properly cited and no modifications or adaptations are made.

© 2022 The Authors. *Alcoholism: Clinical & Experimental Research* published by Wiley Periodicals LLC on behalf of Research Society on Alcoholism.

INTRODUCTION

Prenatal alcohol exposure (PAE) is a significant public health concern. PAE is detrimental to the growth of the developing fetus, often resulting in a constellation of negative infant outcomes, including craniofacial dysmorphology, growth retardation, and neurobehavioral abnormalities, which are collectively termed Fetal Alcohol Spectrum Disorders (FASD; Riley & McGee, 2005). The prevalence of FASD ranges from 1.1% to 5% of the school-age population in the United States, while the prevalence of Fetal Alcohol Syndrome (FAS), the severe end of the FASD continuum, varies from 0.05% to 0.2% in the United States (May et al., 2018; May & Gossage, 2001). However, two separate studies, in Texas (Bakhireva et al., 2017) and West Virginia (Umer et al., 2020), assessing a blood metabolite of alcohol in newborn infants, both estimated the prevalence of third-trimester PAE at greater than 8%, suggesting that previous prevalence measures of FASD may actually be underestimated. FASD remains difficult to prevent due to high rates of unplanned pregnancies and alcohol consumption patterns in women of childbearing age. Approximately half of the pregnancies in the United States are unplanned (Finer & Zolna, 2016) and ~18% of women report alcohol consumption during early pregnancy (SAMHSA, 2013). There is clearly a need for greater research into interventions that address the effect PAE has on a developing fetus.

PAE affects various developing organs and tissues, leading to the pleiotropic effects seen in FASD. *Ex vivo* modeling of early embryonic and fetal development using rodent and primate-derived embryonic stem cells (ESCs) has shown that ethanol (EtOH) induces apoptosis and influences proliferation within these cells (Arzumayan et al., 2009; Nash et al., 2009; VandeVoort et al., 2011). ESC studies indicate that EtOH impairs differentiation of stem cells toward a number of developmental lineages (Adler et al., 2006; Krishnamoorthy et al., 2013; VandeVoort et al., 2011). Previous studies in cells committed to neural lineages shows that while more mature developing neurons are susceptible to apoptosis following EtOH exposure (Cheema et al., 2000b; Mooney & Miller, 2001, 2003), neural stem, and progenitor cells are resistant to apoptosis (Prock & Miranda, 2007), but are nevertheless depleted due to increased proliferation and premature maturation (Camarillo & Miranda, 2008; Miller, 1996; Miller & Nowakowski, 1991; Salem et al., 2021a, 2021b; Santillano et al., 2005). Our recent studies indicate that some of the premature maturation effects of developmental EtOH exposure may be mediated by miRNAs secreted from neural stem cells (NSCs) in nanometer-sized extracellular vesicles (EVs; Tseng et al., 2019).

EVs represent an exciting and novel means of intercellular communication and transfer of macromolecules including proteins and nucleic acids, and can serve as both biomarkers for disease and therapeutic delivery vehicles. Mesenchymal stem cell-derived EVs have been demonstrated to minimize damage and cognitive deficits due to traumatic brain injury and epilepsy (Kim et al., 2016a; Long et al., 2017). Recently, the capsid forming protein Arc has been identified in neuron-derived EVs, and found to transport its own mRNA between neurons (Ashley et al., 2018; Pastuzyn et al., 2018). Arc is a

member of a large class of gag-like proteins (GLPs) encoded in the genome (Campillos et al., 2006), that may also be biologically active in neural tissues, and have the potential to be packaged in EVs, and transported to recipient cells to influence their biology.

GLPs are encoded by genetic remnants of endogenous retroviruses (ERVs), which became trapped in the eukaryotic genome. The primary components of a retrovirus are long terminal repeats that border the central components of *gag*, *pol*, and *env* (Kaneko-Ishino & Ishino, 2012). These components of ERVs may retain some aspect of their original viral function that the host has since adapted for its own survival (Kaneko-Ishino & Ishino, 2012). For example, Arc retains its original GLPs ability to interact with mRNAs and package these mRNAs in capsid-like structures for membrane-bound export in EVs, including Arc mRNA (Ashley et al., 2018; Pastuzyn et al., 2018). Aside from Arc, there may be other GLPs encoded in the genome capable of packaging RNAs into capsid-like structures within EVs. Understanding the biology of these GLPs may facilitate an understanding of disease etiology.

GLPs have been identified as crucial factors in developmental processes (Abed et al., 2019; Ashley et al., 2018; Chen et al., 2015; Hishida et al., 2007; Lux et al., 2005), and the *Mammalian Retrotransposon (MART)* family of GLP proteins, derived from the Ty3/Gypsy retrotransposon family, have been found to be highly expressed in the developing fetus, including the brain (Brandt et al., 2005). These data show that GLPs are highly expressed in the fetal brain and likely play a role in neural development and, perhaps, in the etiology of FASD. However, except for Arc, little is known about other GLPs that are highly expressed in the fetal brain; therefore, there is a need to understand the mechanisms and pathways in which they participate (Pandey et al., 2014). For this reason, we assessed the expression of GLPs in cultured neural progenitors derived from fetal mouse brain, and found that 2 GLPs, paternally expressed gene 10 (PEG10) and paraneoplastic antigen MA2 (PNMA2) are present in NSCs and in EVs secreted by NSCs. Moreover, NSC levels of these two GLPs were also significantly increased following EtOH exposure. Using loss-of-function and computational strategies, we present evidence that PEG10 promotes neuronal or astrocytic differentiation, and that both PEG10 and PNMA2 have an anti-apoptotic role in NSCs. We hypothesize that the elevated expression of PEG10 and PNMA2 may be a protective adaptation in NSCs to preserve neuronally directed maturation following EtOH exposure.

MATERIALS AND METHODS

Ex vivo fetal mouse neurosphere culture model

All procedures were performed in accordance with Texas A&M Institutional Animal Care and Use Committee guidelines and approval. C57BL/6J (Ai14) mice (Jackson Laboratories, Catalog # 007914) were bred in-house and timed mated overnight with the following morning following mating set as gestational day (GD) 0.5. NSCs were collected from the dorsal telencephalic vesicles of GD

12.5 mouse fetuses. At the time of collection, fetal sex was determined as we have previously reported (Salem et al., 2021a). Briefly, genomic DNA, derived from fetal tail samples using alkaline lysis, underwent a rapid qPCR protocol using primers to detect repetitive sequences on the X (Kunieda et al., 1992) and Y (Itoh et al., 2015) chromosomes. Cortical neuroepithelial tissues within a single pregnancy were pooled by sex. Male and female fetal NSCs were separately propagated as nonadherent spheroids in serum-free mitogenic media, as previously published (Camarillo et al., 2007; Prock & Miranda, 2007; Santillano et al., 2005; Sathyan et al., 2007; Tsai et al., 2014).

EtOH treatment

NSCs were seeded at a density of 2×10^6 cells per T25 flask (Corning; Catalog # 353082), with each flask being defined as a single sample, and were randomly assigned to a control (0 mg/dl, 0 mM), moderate (120 mg/dl, 26 mM), or high (320 mg/dl, 70 mM) EtOH exposure group. The EtOH concentration was chosen based on blood alcohol concentrations attainable either during binge drinking (120 mg/dl), or by adults with chronic alcohol use disorders (320 mg/dl; Adachi et al., 1991). Before use, 190 proof EtOH (Koptec-Decon Labs; Catalog # V1101) was diluted into fresh culture medium, and EtOH concentrations in culture-conditioned medium were measured by gas chromatography (Thermo Fisher; Trace 1310) for each experiment. Both control and EtOH-treated flasks were tightly capped and parafilm sealed, to prevent EtOH loss in the culture medium throughout the 5-day exposure period. Gas chromatographic analyses of our EtOH exposure groups indicated that alcohol concentrations in the media (97 to 139 mg/dl, 21 to 30 mM for moderate dose and 273 to 346 mg/dl, 59 to 75 mM for high dose) approximated the blood alcohol concentration attained in binge drinkers and in heavy drinkers, respectively (Adachi et al., 1991; Perper et al., 1986). Mitogen-withdrawal-driven differentiation was facilitated by seeding neurospheres onto laminin-coated (Thermo Fisher; Catalog # 23017015) culture dishes in the absence of EGF and LIF, but with FGF, resulting in the preferential formation of neuronal-lineage-committed migratory cells, as described previously (Camarillo et al., 2007; Camarillo & Miranda, 2008; Miranda et al., 2008).

EV isolation

Culture-conditioned media were collected from control and EtOH-treated neurosphere cultures and passed through a 0.2 μ m of sterile filter with polyethersulfone membrane (VWR; Catalog # 28145-501) to exclude particles with diameters larger than 200 nm. Filtered media was then concentrated using a 100 kDa MWCO centrifugal filter (Pall; Catalog # MAP100C38) according to manufacturer's recommendations. EVs were isolated using ultracentrifugation (Théry et al., 2006). Briefly, after pelleting cells and debris, EVs were pelleted at $100,000 \times g$ for 70 min and washed with PBS before final

isolation of EVs at $100,000 \times g$ for 70 min. Previously, we showed that this method resulted in the successful isolation of EVs ranging in size from 50 to 200 nm, with a diameter median of ~130 nm, and were able to visualize these EVs with transmission electron microscopy (Tseng et al., 2019).

Western blot analysis

Protein from mouse neurospheres and EVs was extracted using $1 \times$ RIPA lysis buffer (EMD Millipore; Reference # 20-188), with addition of Halt Protease and Phosphatase Inhibitor Cocktail (Thermo Fisher Scientific; Product # 78442). Extracted protein concentration was determined using Pierce BCA Protein Assay Kit (Thermo Fisher Scientific; Catalog # 23225). Ten micrograms of protein were size-fractionated on a 4% to 12% Bis-Tris Gel (Life Technologies; Catalog # NP0329BOX), at 200V for 50 min, and blotted to a PVDF membrane using iBlot Transfer System (Thermo Fisher Scientific; Catalog # IB301001). The blot was then incubated in Revert™ 700 Total Protein Stain for Western Blot Normalization (LI-COR, Lincoln, NE; Catalog # 926-11011) and washed according to manufacturer's recommendations. Subsequently, the membrane was blocked for 1 h at room temperature with agitation with Intercept® (TBS) Protein-Free Blocking Buffer (LI-COR; Catalog # 927-80001), then incubated overnight at 4°C with agitation with polyclonal rabbit anti-PEG10 antibodies diluted at 1:1000 (Abcam; Catalog # ab181249) and mouse anti-PNMA2 antibodies diluted to 1:1000 (Santa Cruz Biotech; Catalog # sc-390762). Antibodies for cell-enriched markers, DREBRIN (Abcam; Catalog # ab60933), NDUFS1 (Abcam; Catalog # ab157221), ATPB (Abcam; Catalog # ab14730), and CALNEXIN (Abcam; Catalog # ab213243), were used at 1:1000 dilutions. An antibody for the EV-enriched marker TSG101 (Santa Cruz Biotech; Catalog # sc-7964), was used at a 1:1000 dilution. The blot was washed and incubated with IRDye® 800CW Goat anti-Rabbit IgG Secondary Antibody (LI-COR; Catalog # 926-32211) at dilution 1:10,000 and IRDye® 680RD Goat anti-Mouse IgG Secondary Antibody (LI-COR; Catalog # 926-68070) at dilution 1:10,000 for 1 h. All blots were visualized using an Odyssey® CLx Imaging System (LI-COR) and blots were analyzed using Image Studio™ Lite Software (LI-COR) and normalized against Revert™ 700 Total Protein Stain, according to manufacturer recommendations. The same composite sample was included on each immunoblot to allow for quantitative comparisons between blots. The composite sample is an equal mixture of protein of all samples to create a standard sample.

siRNA transfection for knockdown

Scrambled siRNA (as control), PEG10 siRNA, and PNMA2 siRNA, at a concentration of 25 nM (Dharmacon siRNA; Scrambled: Catalog #D-001206-13-05, PEG10: Catalog #M-055648-01-0005, PNMA2: Catalog #M-051324-01-0005), were transfected into NSCs, using

Lipofectamine RNAiMAX (Thermo Fisher; Catalog # 13778) according to the manufacturer's recommendations.

MTT cell viability assay

The 3-(4,5-dimethylthiazol-2-yl)-2,5-diphenyltetrazolium bromide (MTT) colorimetric assay (Thermo Fisher; Catalog # M6494) for cell metabolic activity, measured by formation of a colored formazan reaction product, was used to assess the number of viable cells. Seventy-two hours following transfection with siRNAs, NSCs were incubated for 3 h with 6 mM of MTT. The reaction product was subsequently solubilized with 10% SDS in 0.01 N of HCl for 3 h. Absorbance intensities were measured at 570 nM, using Tecan Infinite 200 Microplate Reader (Tecan; SKU# 8344-50-0005).

Cell death analysis

At 48 h post-transfection with siRNAs, the Promega Caspase-Glo[®] 3/7 Assay Systems (Promega; Catalog # G8091) were used to quantify apoptotic cell death according to the manufacturer's instructions and results were quantified on a plate reader (Tecan).

Cell cycle analysis

At 48 h post-transfection with siRNAs, DNA synthesis was assessed by pulse-labeling cells with 10 μ M of EdU (5-ethynyl-2'-deoxyuridine) for 1 h. Cells were immediately harvested, and cell cycle analysis was performed with the Click-iT[®] EdU Alexa Fluor[®] 488 Flow Cytometry

Assay Kit (Thermo Fisher; Catalog # C10420), in conjunction with 7-Amino-Actinomycin D (Thermo Fisher; Catalog # 00-6993-50), according to the manufacturer's recommendations. Rates of incorporation were determined using the Beckman Coulter[®] Gallios 2/5/3 Flow Cytometer. Data were analyzed using Kaluza software (Beckman Coulter).

RNA isolation and mRNA qPCR

Total RNA from mouse neurospheres was isolated using the miRNeasy mini kit (Qiagen; Catalog # 217004). cDNA synthesis was performed using the qScript[™] cDNA SuperMix (Qiagen; Catalog # 95048). qPCR was performed using a 10 μ l mix of cDNA, PerfeCTa[®] SYBR[®] Green FastMix[®], ROX[™] (Quanta Bio; Catalog # 95073-250), and gene appropriate primers (Table 1). qPCR analysis was performed on an Applied Biosystem ViiA 7 Real-time PCR system (ABI/Life Technologies). RNA expression values of mean $2^{-\Delta\Delta CT}$ were normalized to β -actin. Primers were designed to span exon-exon junctions and for each primer pair, thermal stability curves were assessed for evidence of a single amplicon. The length of each amplicon was verified using agarose gel electrophoresis, and amplicon identity was verified by Sanger sequencing.

Data analysis of scRNA sequencing

PEG10 deletion is embryonically lethal (Ono et al., 2006); therefore, virtual KO analysis was conducted on data obtained from our single cell RNA sequencing (scRNA-seq) of GD14.5 control cerebral cortex (NCBI GEO accession number GSE158747; Salem et al., 2021a),

TABLE 1 List of primers used

Target (<i>mus musculus</i>)	Forward sequence	Reverse sequence	Product size (bp)	NCBI accession number
<i>Peg10</i>	CCCTCATCCTTCGTGGCATC	GTGGTTGGCGTCTTTTGTT	77	NM_130877
<i>Pnma2</i>	GACACTCCACCCGCTAATGG	GGCTGGTTGTTGTAACGCG	365	NM_175498
<i>Nes</i>	CTCAGATCCTGGAAGGTGGG	GCAGAGTCTGTATGTAGCCA	81	NM_016701
<i>Olig2</i>	GAACCCCGAAAGGTGTGGAT	TTCCGAATGTGAATTAGATTTGAGG	105	NM_016967
<i>Rbfox3/NeuN</i>	AACCAGCAACTCCACCCTTC	CGAATTGCCGAACATTTGC	118	NM_001285437
<i>Pdgfra</i>	CGTGCTTGGTCGGATTTTGG	CAGGTTGGGACCGCTTAAT	83	NM_001083316
<i>Gfap</i>	CTGAGGCAGAAGCTCCAAGAT	CTCCAAATCCACACGAGCCA	111	NM_001131020
<i>Glast</i>	CCATGTGCTTCGGTTTCGTG	CCAGAGGCGCATACCACATTA	126	NM_148938
<i>Actb</i>	CTCTGGCTCTAGCACCATGAAGA	GTA AACG CAGCTCAGTAACAGTCCG	200	NM_007393
<i>Arl6ip1</i>	GTTTCGCTCGTTGATAACCGC	AAGACTTGCAGTCTCCACGG	89	NM_019419
<i>Ube2c</i>	AGCCGGCACCCTATATGAAG	GCAGCGTGTGTGTTCAAAGG	252	NM_026785
<i>Actg1</i>	GCCGCCGGCTTACACT	CTCGTACCCACGTATGAGT	235	NM_009609
<i>H3f3a</i>	CCTCGGTGTCAGCCATCTTT	GCCATGGTAAGGACACCTCC	140	NM_008210
<i>Tmsb4x</i>	AGCACACATAAAGCGGCGT	ATTCGCCAGCTTGCTTCTCT	239	NM_021278
<i>Tuba1a</i>	CCATCCACCCGGCAGC	TCTCTCCCCCAATGGTCTT	168	NM_011653
<i>Ubb</i>	GCAAGGAGGTTTCCAGAGCTT	CCAATTAGGCGTTTTTGCCGA	180	NM_011664

as described in Osorio et al. (2022), to determine potential gene targets that would be impacted in the developing fetal mouse brain if PEG10 or PNMA2 were to be deleted. Data analysis from our previously published dataset focused on those cell clusters that most closely resemble the ventricular zone (VZ), the subventricular zone (SVZ), and transient progenitor cells (TPC; Salem et al., 2021a), as these are the cell populations that are most closely recapitulated in our neurosphere model. These predicted altered genes were then compared to genes identified as EtOH-sensitive and as hub genes in WGCNA analysis of the VZ, SVZ, and TPC clusters to identify any overlap and potential network consequences of altered PEG10 and PNMA2 expression in the developing fetal mouse VZ, SVZ, and TPC. Pathway analysis of WGCNA modules was conducted using *Enrichr* (Chen et al., 2013; Kuleshov et al., 2016).

Statistical analysis

Statistical analyses were conducted using the GraphPad Prism software, version 9 for Windows. Results are expressed as the mean \pm SEM. The overall group effects were analyzed for significance using three-way and two-way ANOVA with Dunnett's multiple comparisons post hoc testing when appropriate (i.e., following a significant group effect or given a significant interaction effect between experimental conditions in two-way ANOVA), to correct for a family-wise error rate. All statistical tests, sample sizes, and post hoc analysis are appropriately reported in the results section. A value of $p < 0.05$ was considered statistically significant and a value of $0.1 < p < 0.05$ was considered as trending toward significance.

RESULTS

EtOH exposure increases PEG10 and PNMA2 expression in differentiating mouse NSCs

GLPs were initially screened to select for those highly expressed in embryonic and fetal rodent brain according to published datasets on NCBI Gene Expression from mouse ENCODE transcriptome data (Yue et al., 2014). Of those, the PEG10 and PNMA2 genetic loci were uniquely identified as containing large CpG islands that overlapped with their promoters and at least two enhancer regions according the UCSC Genome Browser (GRCm38/mm10), suggesting they may be sensitive to epigenetic modifications as a result of EtOH exposure. For these reasons, we focused on PEG10 and PNMA2 for our studies.

For PEG10 isoform 1, there was a significant increase in expression as differentiation progressed, represented by day of differentiation, $F(2, 48) = 5.071$, $p = 0.010$, but only a trend of an interaction effect for independent variables sex, treatment, and day, "Sex by Treatment by Day," $F(4, 48) = 2.150$, $p = 0.089$, as a result of EtOH exposure (Figure 1C). EtOH exposure significantly increased the protein expression of PEG10 isoform 2, $F(2, 24) = 10.577$, $p = 0.00370$,

and expression of this isoform increased with maturation, $F(2, 48) = 12.186$, $p < 0.0001$ (Figure 1D), as revealed by 3-way ANOVA. For PNMA2, EtOH exposure resulted in a significant interaction effect for "Treatment by Day", $F(4, 48) = 2.643$, $p = 0.045$, as well as a significant interaction for "Sex by Treatment by Day", $F(4, 48) = 4.649$, $p = 0.003$ (Figure 1E). For PEG10 isoform 1, PEG10 isoform 2, and PNMA2, we observed no sex differences in control but EtOH exposure unmasked sex-specific responses with expression peaking on differentiation day 1 in female NSCs exposed to 320 mg/dl EtOH.

PNMA2 and the PEG10 isoform 1 are present in EVs isolated from mouse NSCs

First, the identity of EVs isolated from male and female NSC-conditioned medium was confirmed using proteins known to be enriched in cells compared to EVs (ATPB, NDUFS1, DREBRIN; Figure 2B). For additional markers confirming the identity of isolated EVs, refer to Figure S1. PNMA2 was confirmed to be present in both EVs and cells consistent with its identity as a GLP. Interestingly, for PEG10, the longer isoform 1 was found to be enriched in EVs compared to cells while the shorter isoform 2 was found to be preferentially enriched in cells. Furthermore, cellular fractionation revealed that PEG10 isoform 2 is predominantly localized in the cytoplasm while PNMA2 is found in both the cytoplasm and nuclear fractions at equivalent levels (Figure S2). However, we observed no significant effects of EtOH exposure on subsequent levels of GLPs in EVs (Figure S3).

Knockdown of PEG10 and PNMA2 promotes apoptosis while not altering cellular metabolism

Given that PEG10 and PNMA2 are both known to be anti-apoptotic (Abed et al., 2019; Chen et al., 2015; Lee et al., 2016; Li et al., 2016; Pang et al., 2018; Peng et al., 2017; Zhang et al., 2017), we investigated whether knockdown of these GLPs would increase apoptosis in NSCs. For efficiency of knockdown of PEG10 and PNMA2, refer to Figure S4. As predicted, we observed an increase in apoptosis following knockdown of both PEG10, $F(1, 16) = 5.058$, $p = 0.039$ (Figure 3A), and PNMA2, $F(1, 16) = 38.11$, $p < 0.0001$ (Figure 3A), compared to scrambled controls. Moreover, there was no significant difference between PNMA2 knockdown and the apoptosis induced by staurosporine, the positive control, $F(1, 16) = 0.110$, $p = 0.745$, suggesting that PNMA2 in particular is important for preventing apoptosis in NSCs. In contrast, for PEG10 knockdown, while it did result in increased apoptosis, the effect was not as severe as that produced by staurosporine, $F(1, 16) = 6.608$, $p = 0.021$ for the comparison with staurosporine. In an ANOVA model including scrambled control and PEG10 knockdown, there was a significant main effect of sex, $F(1, 16) = 8.237$, $p = 0.011$, with male-derived NSCs in each case exhibiting higher levels of caspase activity. In no other ANOVA analysis models was there a significant main effect of sex or interaction effects.

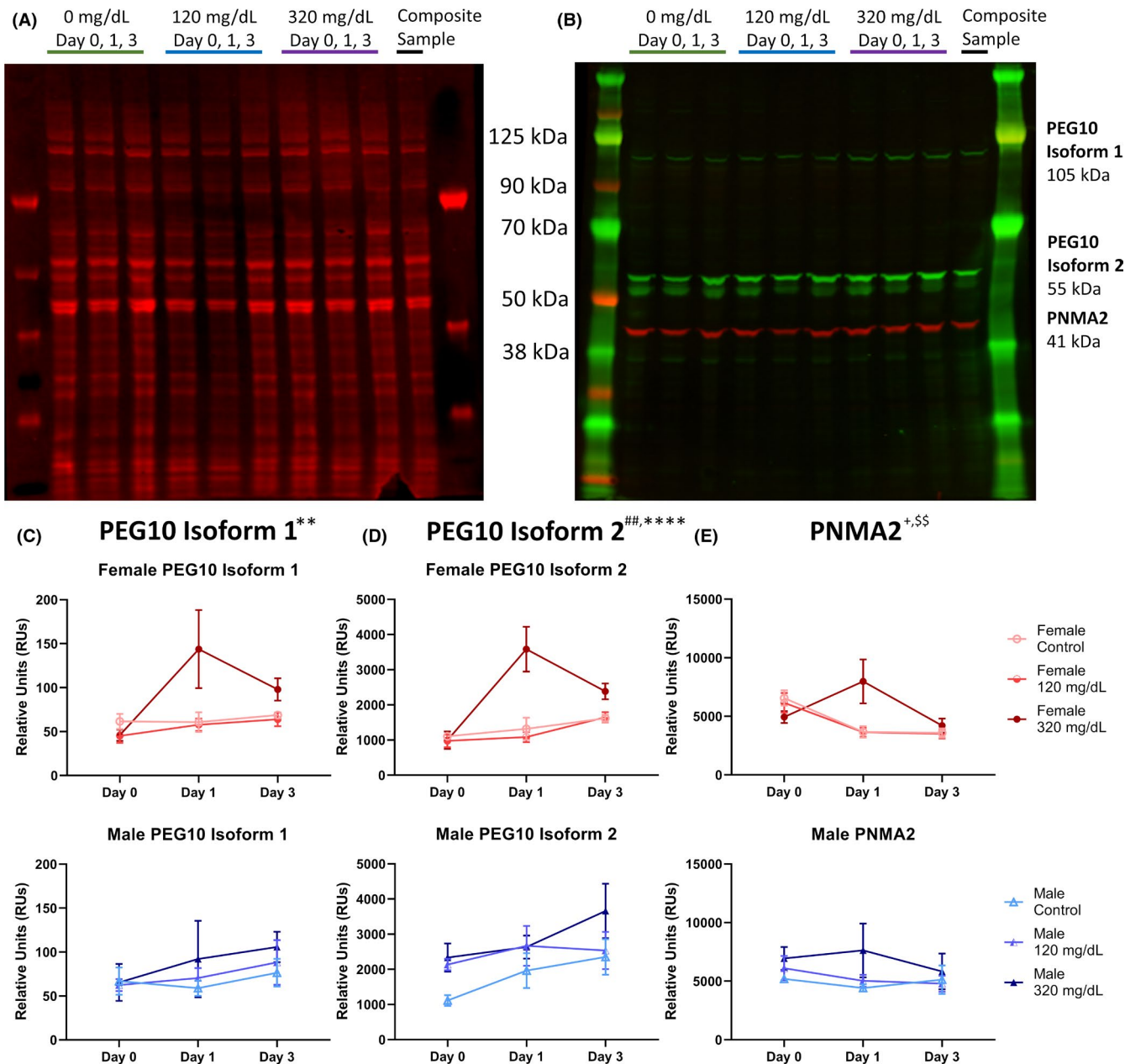


FIGURE 1 Previous EtOH exposure increases PEG10 and PNMA2 protein expression during early differentiation of NSCs. Representative western immunoblots (A) stained for total protein and (B) with antibodies (green fluorescence) to PEG10 isoforms 1 and 2 and antibodies (red fluorescence) to PNMA2. Quantitative analysis of relative protein levels of (C) PEG10 isoform 1, (D) PEG10 isoform 2, and (E) PNMA2 on Days 0, 1, and 3 of early differentiation of NSCs. The same composite sample (see methods) was included on each immunoblot to allow for comparisons between blots. $n = 5$ samples per group. # = main effect of Treatment, * = main effect of Day, + = interaction effect, "Treatment by Day," \$ = interaction effect, "Sex by Treatment by Day." Significance was determined using 3-way ANOVA. # $p < 0.05$, ## $p < 0.01$, ### $p < 0.0001$

Additionally, we investigated whether knockdown of PEG10 and PNMA2 has an impact on cellular metabolism and observed no difference in NADPH-dependent metabolism between PEG10, $F(1, 16) = 0.037$, $p = 0.850$ (Figure 3B), and PNMA2, $F(1, 16) = 0.007$, $p = 0.934$ (Figure 3B), compared to scrambled control. We next investigated whether knockdown of PEG10 and PNMA2 impacted cell cycle progression. While an increased proportion of cells in G1/G0 phase was observed in PEG10 knockdown with a trend toward significance, $F(1, 16) = 4.194$, $p = 0.057$

(Figure 4A), no differences were found between PEG10 knockdown and scrambled control for G2/M phase, $F(1, 16) = 0.511$, $p = 0.485$, or S phase, $F(1, 16) = 2.021$, $p = 0.174$. We also found no difference between PNMA2 knockdown and scrambled control for G1/G0 phase, $F(1, 16) = 1.629$, $p = 0.220$, and G2/M phase ($F(1, 16) = 0.577$, $p = 0.458$, and only a trend toward significance for S phase, $F(1, 16) = 3.275$, $p = 0.089$, outcomes which are collectively consistent with lack of effect on NADPH-dependent cellular metabolism.

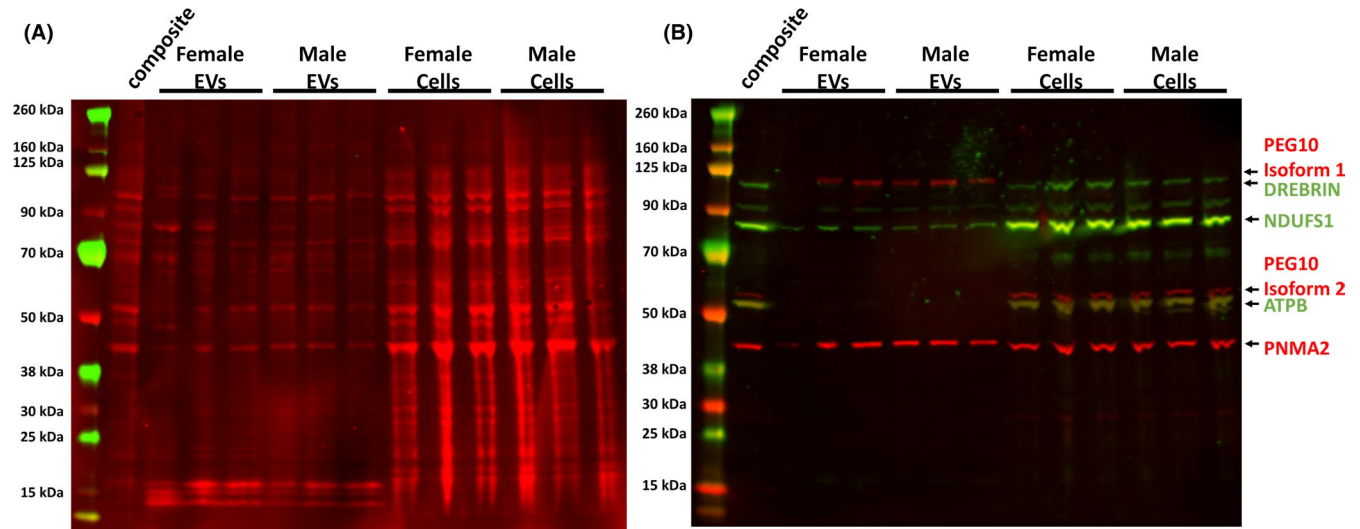


FIGURE 2 PEG10 and PNMA2 are present in EVs. (A) Total protein stain of male and female NSCs and EVs isolated from culture media of the NSCs. (B) Immunoblot showing presence of GLPs in red and presence of cell-enriched proteins (anti-DREBRIN, NDUFS1, and ATPB antibodies) in green

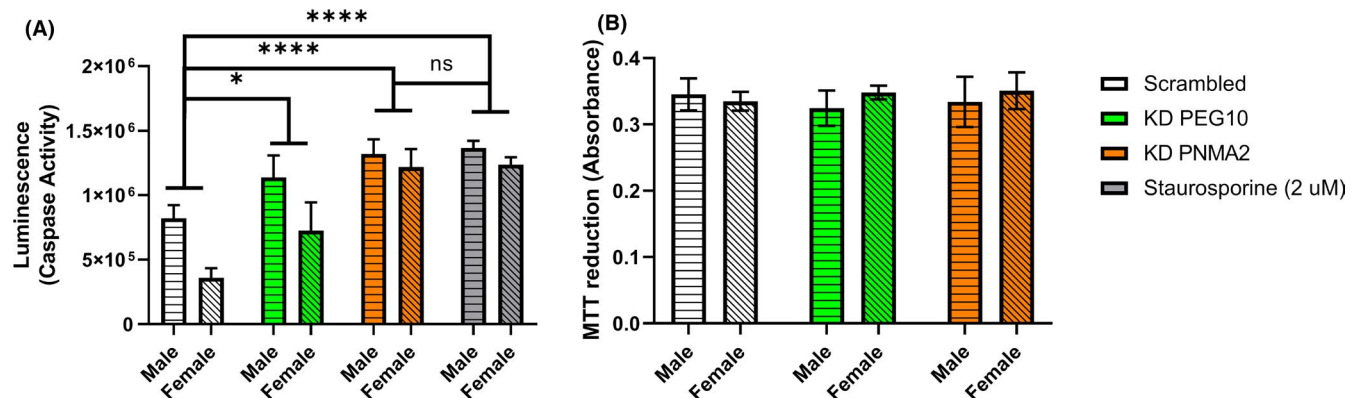


FIGURE 3 PEG10 and PNMA2 are anti-apoptotic and do not affect cellular metabolism. (A) Quantification of caspase 3/7 activity by luciferase assay following PEG10 and PNMA2 knockdown. (B) MTT absorbance values following knockdown of PEG10 and PNMA2 in NSCs. $n = 5$ samples per group. * = main effect of Treatment by 2-way ANOVA. * $p < 0.05$, **** $p < 0.0001$

PEG10 knockdown decreases neuronal and astrocytic lineage markers

To investigate potential impact on lineage-specific maturation of NSCs, PEG10 and PNMA2 were knocked down and transcripts associated with neuronal (*Rbfox3/NeuN*, *Nes*), oligodendrocytic (*Olig2*, *Pdgfra*), and astrocytic (*Gfap*, *Glial*) lineages were quantified. For PEG10 knockdown, there was a significant decrease in *Rbfox3/NeuN*, $F(1, 15) = 5.585$, $p = 0.032$ (Figure 5A), and *Glial*, $F(1, 16) = 6.019$, $p = 0.026$ (Figure 5F), and a trend toward a significant decrease in *Gfap*, $F(1, 16) = 3.893$, $p = 0.066$ (Figure 5E). Trends toward a significant decrease for *Nes*, $F(1, 16) = 3.909$, $p = 0.066$ (Figure 5B), and *Pdgfra*, $F(1, 16) = 3.076$, $p = 0.099$ (Figure 5D), were observed but no difference was observed for *Olig2*, $F(1, 16) = 1.010$, $p = 0.330$ (Figure 5C). For PNMA2 knockdown, only an interaction effect was observed for *Nes* mRNA, $F(1, 16) = 7.524$, $p = 0.0144$ (Figure 5B), with an increase observed in female fetal-derived NSCs, but not in NSCs

derived from male fetuses. Otherwise, a trend toward significant increase for *Rbfox3/NeuN*, $F(1, 15) = 3.415$, $p = 0.084$ (Figure 5A), was seen and no difference was observed in transcripts for *Olig2*, $F(1, 16) = 0.111$, $p = 0.744$ (Figure 5C), *Pdgfra*, $F(1, 16) = 0.0999$, $p = 0.756$ (Figure 5D), *Gfap*, $F(1, 16) = 0.187$, $p = 0.672$ (Figure 5E), and *Glial*, $F(1, 16) = 1.703$, $p = 0.210$ (Figure 5F).

scRNA-seq analysis of fetal mouse ventricular zone cells reveals potential consequences of knockout of PEG10 and PNMA2

To investigate the consequences of region-specific KO of PEG10 and PNMA2, virtual KO using *scTenifoldKnk* (Osorio et al., 2022) was performed on control GD14.5 fetal mouse cerebral cortical cells from our previously published scRNA-seq dataset (Salem et al., 2021a; GSE158747). *scTenifoldKnk* used scRNA-seq data

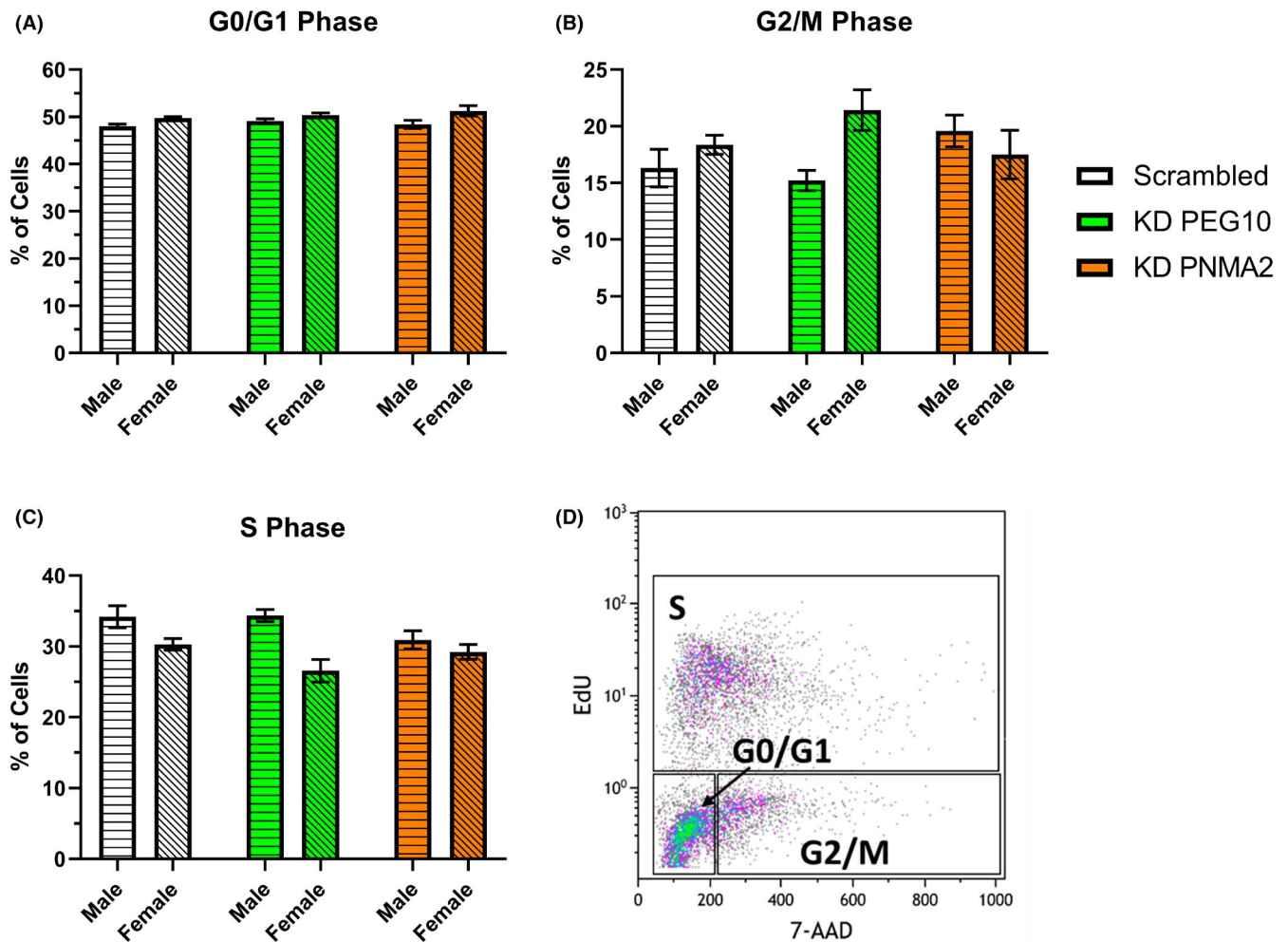


FIGURE 4 PEG10 and PNMA2 do not influence cell cycle dynamics in NSCs. Proportion of cells in (A) G0/G1, (B) G2/M, or (C) S phase of the cell cycle following PEG10 and PNMA2 siRNA-mediated knockdown. (D) Representative flow cytometry image. For panel (A), mean \pm SEM for each group is as follows: Scrambled Male = 48.00% \pm 0.45, Scrambled Female = 49.75% \pm 0.26, KD PEG10 Male = 49.11% \pm 0.46, KD PEG10 Female = 50.37% \pm 0.48, KD PNMA2 Male = 48.41% \pm 0.45, KD PNMA2 Female = 51.27% \pm 1.09. $n = 5$ samples per group

from the control samples in GSE158747 to construct a single-cell gene regulatory network (scGRN). Then, the two GLPs of interest, *Peg10*, or *Pnma2* were each “knocked out” from the constructed scGRN by setting weights of the gene’s outward edges to zeros. The “pseudo-KO” scGRN is compared with the original scGRN to predict genes whose expression and regulatory relationship will be perturbed. These analyses showed that virtual KO of *Peg10* is predicted to alter expression of 28 genes (Figure 6A; Table S1) and virtual KO of *Pnma2* altered expression of 23 genes (Figure 6B; Table S2). To assess potential repercussions of altered PEG10 and PNMA2 expression resulting from EtOH exposure, these lists of genes were compared to the hub genes identified in WGCNA analysis and also identified as EtOH sensitive (Salem et al., 2021a). Only clusters identified as being part of the VZ, SVZ, and TPC were considered as these are the most similar to the niche represented by our neurosphere model (Figure 6C) and *Peg10* and *Pnma2* were also most highly expressed in SVZ and VZ of the neurogenic fetal mouse neocortex. For genes altered by virtual KO of *Peg10*, three

modules of male cells and two modules of female cells were identified as having hub genes (*Arl6ip1*, *Dbi*, *Ube2c*, *H2afz*) that are also predicted to be impacted by alteration in PEG10 expression (Table 2). *Arl6ip1*, $F(1, 16) = 4.600$, $p = 0.0001$, and *Ube2c*, $F(1, 16) = 6.702$, $p = 0.020$, were both significantly downregulated in NSCs after *Peg10* knock down (Figure S5), supporting virtual KO predictions. Primary pathways of these gene modules were cell cycle and mRNA processing related. For genes altered by virtual KO of *Pnma2*, five modules of male cells and eight modules of female cells were identified as having hub genes (*Ubb*, *H3f3a*, *Actg1*, *Tuba1a*, *Tmsb4x*) potentially impacted by alteration in PNMA2 expression (Table 3). *Tuba1a* was significantly increased, $F(1, 16) = 8.864$, $p = 0.009$, and *Ubb* was marginally increased, $F(1, 16) = 3.364$, $p = 0.085$, in NSCs after *Pnma2* knock down, while *Actg1*, *H3f3a*, and *Tmsb4x* were not significantly altered (all p -values > 0.5 ; Figure S6). *Ubb* was the most common hub gene, present in eight modules. Moreover, in an analysis on 123 differentially expressed genes previously identified in *Ubb* knockout

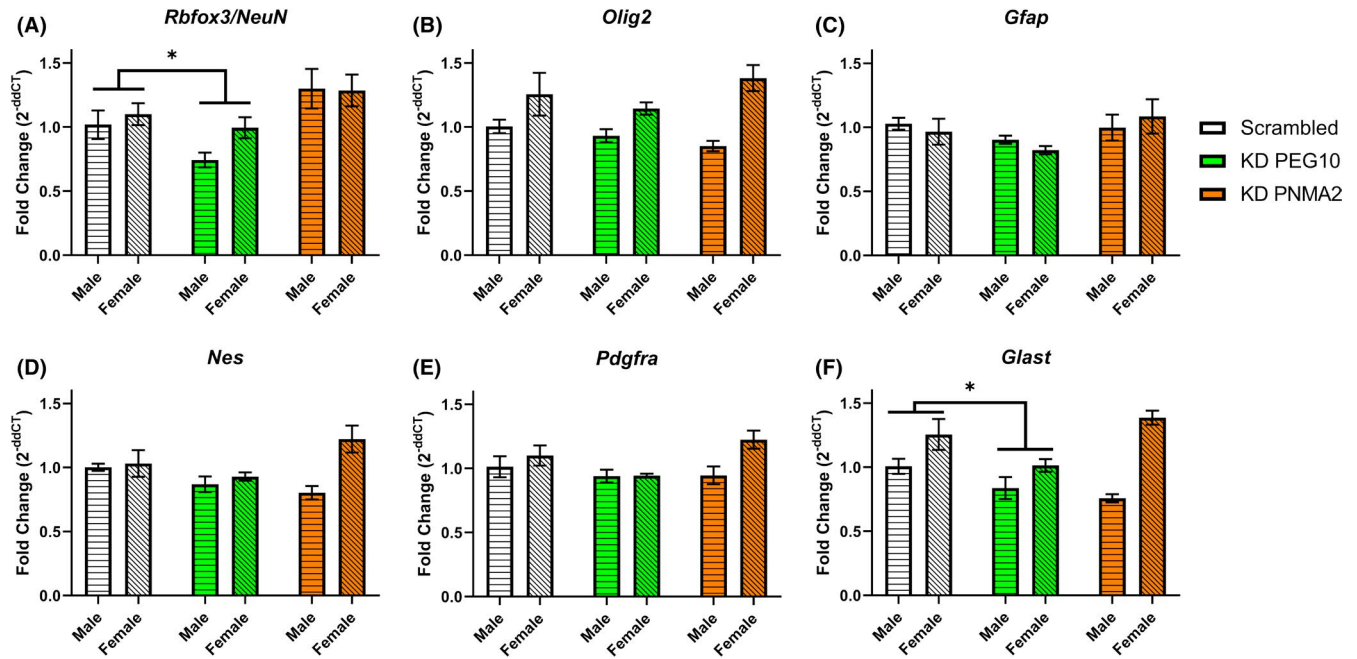


FIGURE 5 PEG10 has a role in neuronal and astrocytic lineage differentiation of NSCs. Expression of (A) *Rbfox3/NeuN*, (B) *Nes*, (C) *Olig2*, (D) *Pdgfra*, (E) *Gfap*, and (F) *Glact* in NSCs following siRNA-mediated knockdown of PEG10 and PNMA2. $n = 5$ samples per group, * = main effect of Treatment by 2-way ANOVA. * $p < 0.05$

murine NSCs (Park et al., 2020), we identified 24 genes that were also significantly alcohol-sensitive within at least one cluster of the VZ, SVZ, or TPC in our previously published single cell RNAseq analysis of the effects of EtOH exposure in the developing fetal cerebral cortex (Salem et al., 2021a; Table S3). Primary pathways implicated by these gene modules with *Ubb* as a hub were “regulation of gene transcription” and “protein turnover.”

DISCUSSION

In this study, GLPs were initially screened to select for those highly expressed in embryonic and fetal rodent brain according to published datasets (Yue et al., 2014). Of those, PEG10 and PNMA2 were uniquely identified as having larger CpG islands that overlapped with their promoters and at least two enhancer regions according to the UCSC Genome Browser (GRCm38/mm10) and as being EtOH sensitive. Both showed increased expression during NSC differentiation after previous EtOH exposure, revealing a persistent change of programming. Additionally, both PEG10 and PNMA2 were present in EVs isolated from NSCs. Specific to PEG10, we identified a predominance of the longer isoform 1 in EVs with the shorter isoform 2 predominating in cells. Moreover, both PEG10 and PNMA2 were shown to be anti-apoptotic in NSCs, as knockdown of these gene transcripts resulted in increased apoptosis, but did not alter cell cycle progression or cellular metabolism. Knockdown of PEG10 decreased the expression of neuronal and astrocytic markers while knockdown of PNMA2 had minimal impact on lineage markers. Sets of genes were predicted to be perturbed by altered PEG10 and PNMA2 expression by virtual KO and specific genes of these

sets were identified as EtOH-sensitive hub genes in gene networks. Moreover, these gene networks contribute to key cellular processes such as cell cycle, mRNA processing, regulating gene transcription, and protein turnover.

Over evolutionary time scales, retroviruses infect, become incorporated into, and permanently encode within vertebrate genomes as ERVs, where they lose the ability to retrotranspose, but acquire new functions and are repurposed by the host organism (Miller et al., 2000). For example, in placenta, one member of this class, PEG10, is highly expressed in trophoblast giant cells, and also in decidual tissues surrounding maternal blood spaces in the labyrinthine zone of the placenta, suggesting an essential role for PEG10 in the maternal-fetal blood system interface (Henke et al., 2013). Genetic deletion of PEG10 is lethal to the early embryo, due to lack of proper placentation and the occurrence of placental defects (Ono et al., 2006). Moreover, it is very likely that GLPs like PEG10 have important roles in developmental processes beyond the placenta as they have been identified as being highly expressed throughout the developing fetus, including in organs like brain, eye, lung, liver, and kidney (Brandt et al., 2005). The impact of developmental alcohol exposure on the function of GLPs during neurogenesis remains to be determined, and was therefore, a focus of this study. A screen of GLPs highly expressed in fetal brain revealed PEG10 and PNMA2 as EtOH sensitive and scRNA-seq revealed these as most highly expressed in SVZ and VZ of second trimester equivalent mouse neocortex. Furthermore, PEG10 and PNMA2 have promoters spanned by large CpG islands with 2 nearby enhancer regions spanned by that same CpG island (Karolchik et al., 2004), supporting the possibility that these genes may be sensitive to epigenetic remodeling such as that attributable

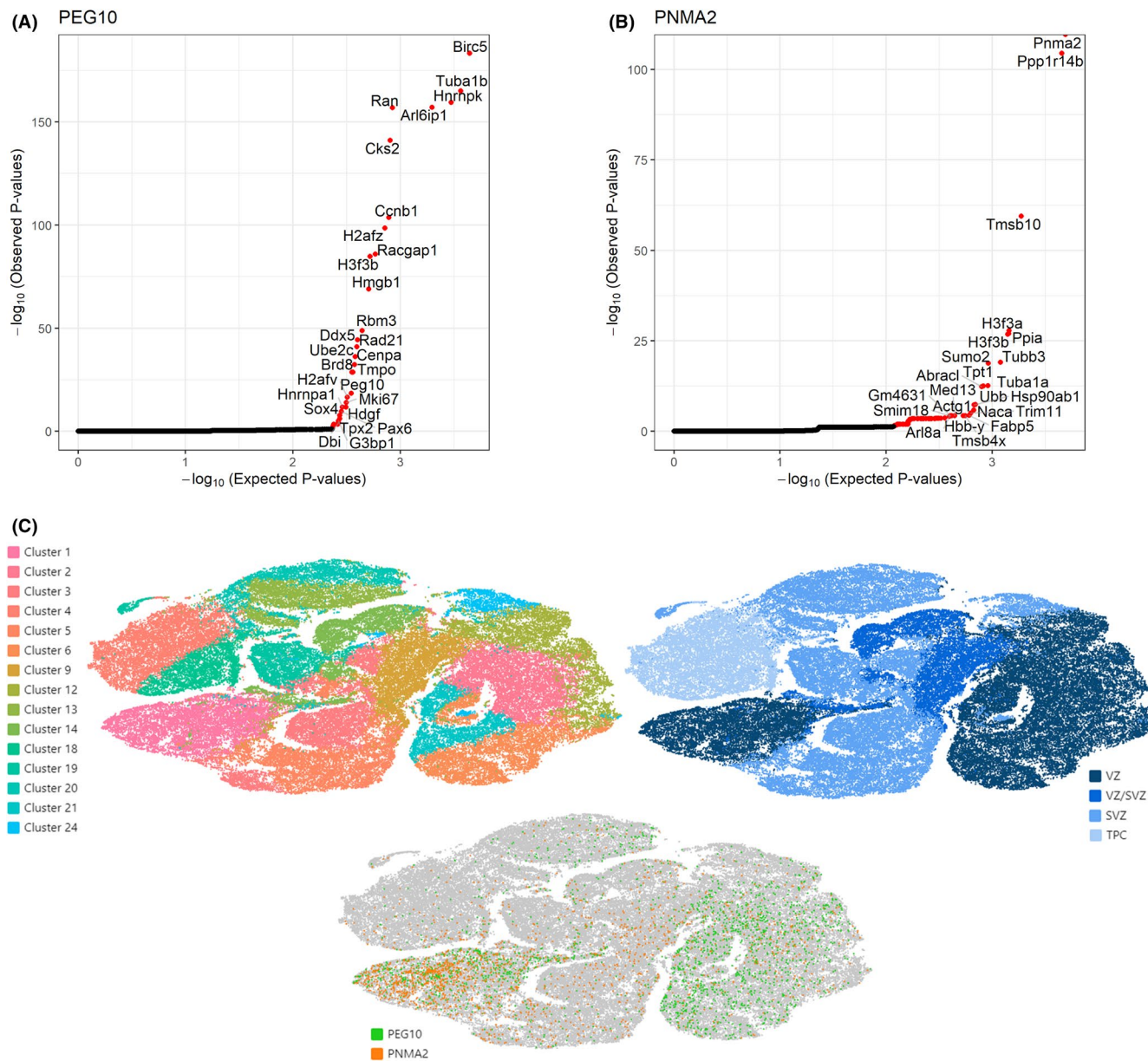


FIGURE 6 Virtual KO reveals genes linked to PEG10 and PNMA2. Genes predicted to have altered expression by virtual KO of (A) *Peg10* and (B) *Pnma2*. (C) PEG10 and PNMA2 transcript expression in GD14.5 fetal mouse VZ, SVZ, and TPC as identified in scRNA-seq

TABLE 2 Modules containing PEG10 Virtual KO targets and dysregulated by EtOH

Cell type	Cluster	Module	Sex	Hub gene	EtOH on hub	Virtual KO enrichment	Enrichr pathway
Ventricular Zone	6	Yellow	Male	Arl6ip1	Down	10 of 28	Cell cycle
Ventricular Zone	2	Yellow	Female	Dbi	Up	2 of 28	Cell-cell adhesion
Ventricular Zone/ Subventricular Zone	14	Blue	Male	Ube2c	Down	11 of 28	Cell cycle
Subventricular Zone	5	Blue	Male	H2afz	Down	14 of 28	mRNA processing
Subventricular Zone	5	Yellow	Female	Ube2c	Up	14 of 28	Capped intron-containing pre-mRNA processing

TABLE 3 Modules containing PNMA2 Virtual KO targets and dysregulated by EtOH

Cell type	Cluster	Module	Sex	Hub gene	EtOH on hub	Virtual KO enrichment	Enrichr pathway
Ventricular Zone	1	Turquoise	Male	Ubb	Down	10 of 23	Gene expression
Ventricular Zone	5	Turquoise	Male	Ubb	Down	6 of 23	Translation
Ventricular Zone	1	Turquoise	Female	Ubb	Up	11 of 23	Gene expression
Ventricular Zone	6	Turquoise	Female	Ubb	Up	16 of 23	Gene expression
Ventricular Zone/ Subventricular Zone	9	Blue	Male	H3f3a	Down	11 of 23	Gene expression
Ventricular Zone/ Subventricular Zone	14	Turquoise	Male	H3f3a	Down	16 of 23	Gene expression
Ventricular Zone/ Subventricular Zone	9	Turquoise	Female	Ubb	Up	10 of 23	Gene expression
Ventricular Zone/ Subventricular Zone	14	Turquoise	Female	Ubb	Up	16 of 23	Gene expression
Subventricular Zone	19	Turquoise	Male	Actg1	Down	15 of 23	Translation
Subventricular Zone	3	Turquoise	Female	Tuba1a	Down	14 of 23	mRNA processing
Subventricular Zone	5	Blue	Female	Ubb	Up	6 of 23	Translation
Subventricular Zone	13	Turquoise	Female	Ubb	Up	17 of 23	Cell cycle
Transient Progenitor Cells	4	Yellow	Female	Tmsb4x	Up	8 of 23	Pathogenic E. coli infection

to prenatal EtOH (Schaffner et al., 2020). Moreover, these CpG islands may explain the differential response to EtOH exposure between male and female NSCs that we observed during our early differentiation paradigm. Higher levels of genome methylation in female mice (Grimm et al., 2019) may make female NSCs more sensitive to excess demethylation that occurs as a result of EtOH exposure (Garro et al., 1991), potentially explaining the heightened sensitivity of GLPs to EtOH exposure prior to differentiation.

PEG10 has been predominantly studied in placental maturation and cancer progression and has been shown to inhibit apoptosis (Chunsong et al., 2006; Hu et al., 2004; Kainz et al., 2007; Okabe et al., 2003), while PNMA2 has been predominantly studied in prostatic and other cancer types, and has also been shown to inhibit apoptosis (Lee et al., 2016; Pang et al., 2018). EtOH induces apoptosis in differentiating and more mature neurons (Cheema et al., 2000a; McAlhany et al., 2000) but not in neural progenitors (Prock & Miranda, 2007; Santillano et al., 2005). PEG10 and PNMA2 may mediate the resistance to EtOH-induced apoptosis in this latter population, since both were increased in neural progenitors following EtOH exposure. Moreover, at least in the case of PEG10, siRNA-mediated knockdown did result in significantly increased caspase activity in neural progenitors, lending further support to the hypothesized role for GLPs in developmental neuroprotection.

GLPs may also influence differentiation. A review of the literature suggests that PEG10 promotes cell and tissue differentiation in tissues like placenta (Abed et al., 2019; Chen et al., 2015) and adipose tissues (Hishida et al., 2007). Here, we report that PEG10 may also promote maturation of neural progenitors, since siRNA-mediated knockdown of *Peg10* resulted in decreased expression of

the neuronal marker *Rbfox3/NeuN*, and astrocytic markers, *Gfap* and *Glast*, though future studies are needed to better understand how these changes impact NSC maturation. Previously, we have shown that EtOH promotes premature maturation of neural progenitors (Santillano et al., 2005). These data then suggest that PEG10 may be a mediator of EtOH-induced premature maturation. Therefore, while PEG10 may prove protective through its prevention of apoptosis, a consequence of that prevention may be promotion of premature differentiation.

The virtual KO of *Pnma2*, based on the perturbation of the gene regulatory network in our GD14.5 mouse cerebral cortical scRNA-seq sample, predicted altered expression of *Ubb*. Interestingly *Ubb* was also identified as a hub gene in multiple gene networks that were also found, according to our scRNA-seq analysis (Salem et al., 2021a), to be commonly dysregulated in ventricular and subventricular zone cell sub-populations, by prenatal EtOH exposure. Moreover, deletion mutations of the *Ubb* gene locus, which encodes a polyubiquitin protein, are associated with Down Syndrome, and with congenital anomalies like cleft palate associated with developmental delay (Andrieux et al., 2007; Gerez et al., 2005) that overlap with FASD phenotypes. Pathways associated with these gene networks for which *Ubb* is a hub are primarily concerned with regulating gene transcription and protein turnover. These are key processes in development and explain the negative fetal outcomes associated with *Ubb* and seen in FASD.

GLPs retain at least a portion of the *gag*-domain, making some capable of functioning like the retroviral Gag protein by binding mRNA and being packaged into EVs. A specific example is activity-regulated cytoskeleton-associated protein (ARC) which binds its

own mRNA and is subsequently packed into EVs to be transported to neighboring neurons where the mRNA is translated and ARC has its normal role in neural plasticity (Ashley et al., 2018; Pastuzyn et al., 2018). Moreover, PEG10 mRNA has been identified in hematopoietic stem and progenitor cell EVs (Stik et al., 2017) and PEG10 protein (isoforms 1 and 2) has been isolated from trophoblast stem cell EVs (Abed et al., 2019). PEG10 protein isolated from EVs has been shown to bind its own mRNA in the 5'- and 3'-UTRs (Segel et al., 2021), to interact with other RNA-binding proteins like ATXN2 and ATXN10, and to associate directly or indirectly with over 3000 developmentally relevant transcripts that are subsequently packaged into EVs with PEG10 (Pandya et al., 2021). Transcripts packaged in EVs with PEG10 are capable of being translated in recipient cells (Segel et al., 2021) and this function of PEG10 is important in neuronal migration in mice (Pandya et al., 2021). It is reasonable to assume then that GLPs have additional important roles in developmental processes that are mediated in part by EV transport. These normal mechanisms may be disturbed by PAE as we have previously shown EV cargo to be EtOH-sensitive, with EtOH exposure altering miRNAs in EVs of neural progenitors (Tseng et al., 2019). However, while we predicted EV cargo of GLPs would change in response to EtOH exposure to reflect changes observed in NSCs, we did not observe this outcome. One possible explanation is that a stressor like EtOH may result in uncoupling of EVs from cells and preferential sequestration of protective or anti-apoptotic factors by parent cells over EVs, to support their use by parent cells. This possible means of cyto-protection needs further investigation but is consistent with our previous observations that EtOH does not kill NSCs (Camarillo & Miranda, 2008; Prock & Miranda, 2007; Salem et al., 2021b; Santillano et al., 2005). However, it should be noted that PEG10 and PNMA2 levels within the EVs did not decline, but rather, were maintained at constant levels. EVs are thought to be a means of cell-to-cell communication (Mathieu et al., 2019), and therefore, the maintenance of GLPs in EVs suggest the possibility that EVs may also provide a protective advantage for the NSC niche as a whole. Future studies should focus on determining how EtOH influences packaging of GLPs in NSC-derived EVs as well as their function in target cells. Ultimately, exploiting the paracrine role of GLPs in EVs may be a means to mitigate the effects of PAE, as has been shown with other pathologies (Bian et al., 2014; Kim et al., 2016b; Wang et al., 2017).

ACKNOWLEDGMENTS

This work was supported by grants from the NIH, R01 AA024659 (RCM), F30 AA027698 (MRP), F31 AA028446 (DDC), and F99 NS113423 (NAS).

CONFLICT OF INTEREST

The authors declare no conflict of interest.

ORCID

Marisa R. Pinson  <https://orcid.org/0000-0001-6477-9285>

Rajesh C. Miranda  <https://orcid.org/0000-0002-8359-892X>

REFERENCES

- Abed, M., Verschuere, E., Budayeva, H., Liu, P., Kirkpatrick, D.S., Reja, R. et al. (2019) The Gag protein PEG10 binds to RNA and regulates trophoblast stem cell lineage specification. *PLoS One*, 14, e0214110.
- Adachi, J., Mizoi, Y., Fukunaga, T., Ogawa, Y., Ueno, Y. & Imamichi, H. (1991) Degrees of alcohol intoxication in 117 hospitalized cases. *Journal of Studies on Alcohol*, 52, 448–453.
- Adler, S., Pellizzer, C., Paparella, M., Hartung, T. & Bremer, S. (2006) The effects of solvents on embryonic stem cell differentiation. *Toxicology in Vitro*, 20, 265–271.
- Andrieux, J., Villenet, C., Quief, S., Lignon, S., Geffroy, S., Roumier, C. et al. (2007) Genotype phenotype correlation of 30 patients with Smith-Magenis syndrome (SMS) using comparative genome hybridisation array: cleft palate in SMS is associated with larger deletions. *Journal of Medical Genetics*, 44, 537–540.
- Arzumayan, A., Anni, H., Rubin, R. & Rubin, E. (2009) Effects of ethanol on mouse embryonic stem cells. *Alcoholism, Clinical and Experimental Research*, 33(12), 2172–2179.
- Ashley, J., Cordy, B., Lucia, D., Fradkin, L.G., Budnik, V. & Thomson, T. (2018) Retrovirus-like gag protein Arc1 binds RNA and traffics across synaptic boutons. *Cell*, 172, 262–274.e11.
- Bakhireva, L.N., Sharkis, J., Shrestha, S., Miranda-Sohrabji, T.J., Williams, S. & Miranda, R.C. (2017) Prevalence of prenatal alcohol exposure in the state of Texas as assessed by phosphatidylethanol in newborn dried blood spot specimens. *Alcoholism, Clinical and Experimental Research*, 41, 1004–1011.
- Bian, S., Zhang, L., Duan, L., Wang, X., Min, Y. & Yu, H. (2014) Extracellular vesicles derived from human bone marrow mesenchymal stem cells promote angiogenesis in a rat myocardial infarction model. *Journal of Molecular Medicine*, 92, 387–397.
- Brandt, J., Schrauth, S., Veith, A.-M., Froschauer, A., Haneke, T., Schultheis, C. et al. (2005) Transposable elements as a source of genetic innovation: expression and evolution of a family of retrotransposon-derived neogenes in mammals. *Gene*, 345, 101–111.
- Camarillo, C., Kumar, L.S., Bake, S., Sohrabji, F. & Miranda, R.C. (2007) Ethanol regulates angiogenic cytokines during neural development: evidence from an in vitro model of mitogen-withdrawal-induced cerebral cortical neuroepithelial differentiation. *Alcoholism: Clinical and Experimental Research*, 31, 324–335.
- Camarillo, C. & Miranda, R.C. (2008) Ethanol exposure during neurogenesis induces persistent effects on neural maturation: evidence from an ex vivo model of fetal cerebral cortical neuroepithelial progenitor maturation. *Gene Expression*, 14, 159–171.
- Campillos, M., Doerks, T., Shah, P.K. & Bork, P. (2006) Computational characterization of multiple Gag-like human proteins. *Trends in Genetics*, 22, 585–589.
- Cheema, Z.F., West, J.R. & Miranda, R.C. (2000a) Ethanol induces Fas/Apo [apoptosis]-1 mRNA and cell suicide in the developing cerebral cortex. *Alcoholism, Clinical and Experimental Research*, 24, 535–543.
- Cheema, Z.F., West, J.R. & Miranda, R.C. (2000b) Ethanol induces Fas/Apo [apoptosis]-1 mRNA and cell suicide in the developing cerebral cortex. *Alcoholism, Clinical and Experimental Research*, 24, 535–543.
- Chen, E.Y., Tan, C.M., Kou, Y., Duan, Q., Wang, Z., Meirelles, G.V. et al. (2013) Enrichr: interactive and collaborative HTML5 gene list enrichment analysis tool. *BMC Bioinformatics*, 14, 128.
- Chen, H., Sun, M., Liu, J., Tong, C. & Meng, T. (2015) Silencing of paternally expressed gene 10 inhibits trophoblast proliferation and invasion. *PLoS One*, 10, e0144845.
- Chunson, H., Yuling, H., Li, W., Jie, X., Gang, Z., Qiuping, Z. et al. (2006) CXC chemokine ligand 13 and CC chemokine ligand 19 cooperatively render resistance to apoptosis in B cell lineage acute and chronic lymphocytic leukemia CD23+CD5+ B cells. *The Journal of Immunology*, 177, 6713–6722.

- Finer, L.B. & Zolna, M.R. (2016) Declines in unintended pregnancy in the United States, 2008–2011. *New England Journal of Medicine*, 374(9), 843–852.
- Garro, A.J., Mcbeth, D.L., Lima, V. & Lieber, C.S. (1991) Ethanol consumption inhibits fetal DNA methylation in mice: implications for the fetal alcohol syndrome. *Alcoholism, Clinical and Experimental Research*, 15, 395–398.
- Gerez, L., De Haan, A., Hol, E.M., Fischer, D.F., Van Leeuwen, F.W., Van Steeg, H. et al. (2005) Molecular misreading: the frequency of dinucleotide deletions in neuronal mRNAs for beta-amyloid precursor protein and ubiquitin B. *Neurobiology of Aging*, 26, 145–155.
- Grimm, S.A., Shimbo, T., Takaku, M., Thomas, J.W., Auerbach, S., Bennett, B.D. et al. (2019) DNA methylation in mice is influenced by genetics as well as sex and life experience. *Nature Communications*, 10, 305.
- Henke, C., Ruebner, M., Faschingbauer, F., Stolt, C.C., Schaefer, N., Lang, N. et al. (2013) Regulation of murine placentogenesis by the retroviral genes Syncytin-A, Syncytin-B and Peg10. *Differentiation*, 85, 150–160.
- Hishida, T., Naito, K., Osada, S., Nishizuka, M. & Imagawa, M. (2007) peg10, an imprinted gene, plays a crucial role in adipocyte differentiation. *FEBS Letters*, 581, 4272–4278.
- Hu, C., Xiong, J., Zhang, L., Huang, B., Zhang, Q., Li, Q. et al. (2004) PEG10 activation by co-stimulation of CXCR5 and CCR7 essentially contributes to resistance to apoptosis in CD19+CD34+ B cells from patients with B cell lineage acute and chronic lymphocytic leukemia. *Cellular & Molecular Immunology*, 1, 280–294.
- Itoh, Y., Mackie, R., Kampf, K., Domadia, S., Brown, J.D., O'Neill, R. et al. (2015) Four Core Genotypes mouse model: localization of the Sry transgene and bioassay for testicular hormone levels. *BMC Research Notes*, 8, 69.
- Kainz, B., Shehata, M., Bilban, M., Kienle, D., Heintel, D., Krömer-Holzinger, E. et al. (2007) Overexpression of the paternally expressed gene 10 (PEG10) from the imprinted locus on chromosome 7q21 in high-risk B-cell chronic lymphocytic leukemia. *International Journal of Cancer*, 121, 1984–1993.
- Kaneko-Ishino, T. & Ishino, F. (2012) The role of genes domesticated from LTR retrotransposons and retroviruses in mammals. *Frontiers in Microbiology*, 3, 262.
- Karolchik, D., Hinrichs, A.S., Furey, T.S., Roskin, K.M., Sugnet, C.W., Haussler, D. et al. (2004) The UCSC table browser data retrieval tool. *Nucleic Acids Research*, 32, D493–D496.
- Kim, D.-K., Nishida, H., An, S.Y., Shetty, A.K., Bartosh, T.J. & Prockop, D.J. (2016a) Chromatographically isolated CD63+CD81+ extracellular vesicles from mesenchymal stromal cells rescue cognitive impairments after TBI. *Proceedings of the National Academy of Sciences*, 113, 170–175.
- Kim, D.K., Nishida, H., An, S.Y., Shetty, A.K., Bartosh, T.J. & Prockop, D.J. (2016b) Chromatographically isolated CD63+CD81+ extracellular vesicles from mesenchymal stromal cells rescue cognitive impairments after TBI. *Proceedings of the National Academy of Sciences of the United States of America*, 113, 170–175.
- Krishnamoorthy, M., Gerwe, B.A., Scharer, C.D., Sahasranaman, V., Eilertson, C.D., Nash, R.J. et al. (2013) Ethanol alters proliferation and differentiation of normal and chromosomally abnormal human embryonic stem cell-derived neurospheres. *Birth Defects Research Part B Developmental and Reproductive Toxicology*, 98, 283–295.
- Kuleshov, M.V., Jones, M.R., Rouillard, A.D., Fernandez, N.F., Duan, Q., Wang, Z. et al. (2016) Enrichr: a comprehensive gene set enrichment analysis web server 2016 update. *Nucleic Acids Research*, 44, W90–W97.
- Kunieda, T., Xian, M., Kobayashi, E., Imamichi, T., Moriwaki, K. & Toyoda, Y. (1992) Sexing of mouse preimplantation embryos by detection of Y chromosome-specific sequences using polymerase chain reaction. *Biology of Reproduction*, 46, 692–697.
- Lee, Y.H., Pang, S.W. & Tan, K.O. (2016) PNMA2 mediates heterodimeric interactions and antagonizes chemo-sensitizing activities mediated by members of PNMA family. *Biochemical and Biophysical Research Communications*, 473, 224–229.
- Li, X., Xiao, R., Tembo, K., Hao, L., Xiong, M., Pan, S. et al. (2016) PEG10 promotes human breast cancer cell proliferation, migration and invasion. *International Journal of Oncology*, 48, 1933–1942.
- Long, Q., Upadhy, D., Hattiangady, B., Kim, D.K., An, S.Y., Shuai, B. et al. (2017) Intranasal MSC-derived A1-exosomes ease inflammation, and prevent abnormal neurogenesis and memory dysfunction after status epilepticus. *Proceedings of the National Academy of Sciences of the United States of America*, 114, e3536–e3545.
- Lux, A., Beil, C., Majety, M., Barron, S., Gallione, C.J., Kuhn, H.-M. et al. (2005) Human Retroviral gag- and gag-pol-like proteins interact with the transforming growth factor-B receptor activin receptor-like kinase 1. *Journal of Biological Chemistry*, 280(9), 8482–8493.
- Mathieu, M., Martin-Jaular, L., Lavie, G. & Thery, C. (2019) Specificities of secretion and uptake of exosomes and other extracellular vesicles for cell-to-cell communication. *Nature Cell Biology*, 21, 9–17.
- May, P.A., Chambers, C.D., Kalberg, W.O., Zellner, J., Feldman, H., Buckley, D. et al. (2018) Prevalence of fetal alcohol spectrum disorders in 4 US communities. *JAMA*, 319, 474–482.
- May, P.A. & Gossage, J.P. (2001) Estimating the prevalence of fetal alcohol syndrome. A summary. *Alcohol Research & Health*, 25, 159–167.
- Mcalhany, R.E. Jr., West, J.R. & Miranda, R.C. (2000) Glial-derived neurotrophic factor (GDNF) prevents ethanol-induced apoptosis and JUN kinase phosphorylation. *Brain Research. Developmental Brain Research*, 119, 209–216.
- Miller, M.W. (1996) Limited ethanol exposure selectively alters the proliferation of precursor cells in the cerebral cortex. *Alcoholism, Clinical and Experimental Research*, 20, 139–143.
- Miller, M.W. & Nowakowski, R.S. (1991) Effect of prenatal exposure to ethanol on the cell cycle kinetics and growth fraction in the proliferative zones of fetal rat cerebral cortex. *Alcoholism, Clinical and Experimental Research*, 15, 229–232.
- Miller, W.J., McDonald, J.F., Nouaud, D. & Anxolabéhère, D. (2000) Molecular domestication—more than a sporadic episode in evolution. In: McDonald, J.F. (Ed.) *Transposable elements and genome evolution*. Dordrecht: Springer Netherlands.
- Miranda, R.C., Santillano, D.R., Camarillo, C. & Dohrman, D. (2008) Modeling the impact of alcohol on cortical development in a dish: strategies from mapping neural stem cell fate. In: Nagy, L.E. (Ed.) *Alcohol: methods and protocols*. Totowa, NJ: Humana Press.
- Mooney, S.M. & Miller, M.W. (2001) Effects of prenatal exposure to ethanol on the expression of bcl-2, bax and caspase 3 in the developing rat cerebral cortex and thalamus. *Brain Research*, 911, 71–81.
- Mooney, S.M. & Miller, M.W. (2003) Ethanol-induced neuronal death in organotypic cultures of rat cerebral cortex. *Brain Research. Developmental Brain Research*, 147, 135–141.
- Nash, R.J., Heimbürg-Molinari, J. & Nash, R.J. (2009) Heparin binding epidermal growth factor-like growth factor reduces ethanol-induced apoptosis and differentiation in human embryonic stem cells. *Growth Factors*, 27, 362–369.
- Okabe, H., Satoh, S., Furukawa, Y., Kato, T., Hasegawa, S., Nakajima, Y. et al. (2003) Involvement of PEG10 in human hepatocellular carcinogenesis through interaction with Slah1. *Cancer Research*, 63, 3043–3048.
- Ono, R., Nakamura, K., Inoue, K., Naruse, M., Usami, T., Wakisaka-Saito, N. et al. (2006) Deletion of Peg10, an imprinted gene acquired from a retrotransposon, causes early embryonic lethality. *Nature Genetics*, 38, 101–106.
- Osorio, D., Zhong, Y., Li, G., Xu, Q., Yang, Y., Hillhouse, A. et al. (2022) scTenifoldKnk: an efficient virtual knockout tool for gene function predictions via single-cell gene regulatory network perturbation. *SSRN Electronic Journal*, 3, 100434.
- Pandey, A.K., Lu, L., Wang, X., Homayouni, R. & Williams, R.W. (2014) Functionally enigmatic genes: a case study of the brain ignorome. *PLoS One*, 9, e88889.

- Pandya, N.J., Wang, C., Costa, V., Lopatta, P., Meier, S., Zampeta, F.I. et al. (2021) Secreted retrovirus-like GAG-domain-containing protein PEG10 is regulated by UBE3A and is involved in Angelman syndrome pathophysiology. *Cell Reports Medicine*, 2, 100360.
- Pang, S.W., Lahiri, C., Poh, C.L. & Tan, K.O. (2018) PNMA family: protein interaction network and cell signalling pathways implicated in cancer and apoptosis. *Cellular Signalling*, 45, 54–62.
- Park, C.-W., Jung, B.-K. & Ryu, K.-Y. (2020) Disruption of the polyubiquitin gene Ubb reduces the self-renewal capacity of neural stem cells. *Biochemical and Biophysical Research Communications*, 527, 372–378.
- Pastuzyn, E.D., Day, C.E., Kearns, R.B., Kyrke-Smith, M., Taibi, A.V., McCormick, J. et al. (2018) The neuronal gene Arc encodes a repurposed retrotransposon gag protein that mediates intercellular RNA transfer. *Cell*, 172, 275–288.e18.
- Peng, Y.-P., Zhu, Y., Yin, L.-D., Zhang, J.-J., Wei, J.-S., Liu, X. et al. (2017) PEG10 overexpression induced by E2F-1 promotes cell proliferation, migration, and invasion in pancreatic cancer. *Journal of Experimental & Clinical Cancer Research*, 36, 30.
- Perper, J.A., Twerski, A. & Wienand, J.W. (1986) Tolerance at high blood alcohol concentrations: a study of 110 cases and review of the literature. *Journal of Forensic Sciences*, 31, 212–221.
- Prock, T.L. & Miranda, R.C. (2007) Embryonic cerebral cortical progenitors are resistant to apoptosis, but increase expression of suicide receptor DISC-complex genes and suppress autophagy following ethanol exposure. *Alcoholism: Clinical and Experimental Research*, 31, 694–703.
- Riley, E.P. & Mcgee, C.L. (2005) Fetal alcohol spectrum disorders: an overview with emphasis on changes in brain and behavior. *Experimental Biology and Medicine*, 230, 357–365.
- Salem, N.A., Mahnke, A.H., Konganti, K., Hillhouse, A.E. & Miranda, R.C. (2021a) Cell-type and fetal-sex-specific targets of prenatal alcohol exposure in developing mouse cerebral cortex. *iScience*, 24(5), 102439.
- Salem, N.A., Mahnke, A.H., Tseng, A.M., Garcia, C.R., Jahromi, H.K., Geoffroy, C.G. et al. (2021b) A novel Oct4/Pou5f1-like non-coding RNA controls neural maturation and mediates developmental effects of ethanol. *Neurotoxicology and Teratology*, 83, 106943.
- S.A.M.H.S.A. (2013) The NSDUH report: 18 percent of pregnant women drink alcohol during early pregnancy. Rockville, MD: U.S. Department of Health & Human Services. <https://www.samhsa.gov/data/sites/default/files/spot123-pregnancy-alcohol-2013/spot123-pregnancy-alcohol-2013.pdf>
- Santillano, D.R., Kumar, L.S., Prock, T.L., Camarillo, C., Tingling, J.D. & Miranda, R.C. (2005) Ethanol induces cell-cycle activity and reduces stem cell diversity to alter both regenerative capacity and differentiation potential of cerebral cortical neuroepithelial precursors. *BMC Neuroscience*, 6, 59.
- Sathyan, P., Golden, H.B. & Miranda, R.C. (2007) Competing interactions between Micro-RNAs determine neural progenitor survival and proliferation after ethanol exposure: evidence from an ex vivo model of the fetal cerebral cortical neuroepithelium. *The Journal of Neuroscience*, 27, 8546–8557.
- Schaffner, S.L., Lussier, A.A., Baker, J.A., Goldowitz, D., Hamre, K.M. & Kobor, M.S. (2020) Neonatal alcohol exposure in mice induces select differentiation- and apoptosis-related chromatin changes both independent of and dependent on sex. *Frontiers in Genetics*, 11, 35.
- Segel, M., Lash, B., Song, J., Ladha, A., Liu, C.C., Jin, X. et al. (2021) Mammalian retrovirus-like protein PEG10 packages its own mRNA and can be pseudotyped for mRNA delivery. *Science*, 373, 882–889.
- Stik, G., Crequit, S., Petit, L., Durant, J., Charbord, P., Jaffredo, T. et al. (2017) Extracellular vesicles of stromal origin target and support hematopoietic stem and progenitor cells. *Journal of Cell Biology*, 216, 2217–2230.
- Théry, C., Amigorena, S., Raposo, G. & Clayton, A. (2006) Isolation and characterization of exosomes from cell culture supernatants and biological fluids. *Current Protocols in Cell Biology*, 30, 3.22.1–3.22.29.
- Tsai, P.-C., Bake, S., Balaraman, S., Rawlings, J., Holgate, R.R., Dubois, D. et al. (2014) MiR-153 targets the nuclear factor-1 family and protects against teratogenic effects of ethanol exposure in fetal neural stem cells. *Biology Open*, 3, 741–758.
- Tseng, A.M., Chung, D.D., Pinson, M.R., Salem, N.A., Eaves, S.E. & Miranda, R.C. (2019) Ethanol exposure increases miR-140 in extracellular vesicles: implications for fetal neural stem cell proliferation and maturation. *Alcoholism: Clinical and Experimental Research*, 43, 1414–1426.
- Umer, A., Lilly, C., Hamilton, C., Baldwin, A., Breyel, J., Tolliver, A. et al. (2020) Prevalence of alcohol use in late pregnancy. *Pediatric Research*, 88, 312–319.
- Vandevoort, C.A., Hill, D.L., Chaffin, C.L. & Conley, A.J. (2011) Ethanol, acetaldehyde, and estradiol affect growth and differentiation of rhesus monkey embryonic stem cells. *Alcoholism, Clinical and Experimental Research*, 35, 1534–1540.
- Wang, N., Chen, C., Yang, D., Liao, Q., Luo, H., Wang, X. et al. (2017) Mesenchymal stem cells-derived extracellular vesicles, via miR-210, improve infarcted cardiac function by promotion of angiogenesis. *Biochimica Et Biophysica Acta - Molecular Basis of Disease*, 1863, 2085–2092.
- Yue, F., Cheng, Y., Breschi, A., Vierstra, J., Wu, W., Ryba, T. et al. (2014) A comparative encyclopedia of DNA elements in the mouse genome. *Nature*, 515, 355–364.
- Zhang, M., Sui, C., Dai, B., Shen, W., Lu, J. & Yang, J. (2017) PEG10 is imperative for TGF- β 1-induced epithelial-mesenchymal transition in hepatocellular carcinoma. *Oncology Reports*, 37, 510–518.

SUPPORTING INFORMATION

Additional supporting information may be found in the online version of the article at the publisher's website.

How to cite this article: Pinson, M.R., Chung, D.D., Mahnke, A.H., Salem, N.A., Osorio, D., Nair, V., et al (2022) Gag-like proteins: Novel mediators of prenatal alcohol exposure in neural development. *Alcoholism: Clinical and Experimental Research*, 46, 556–569. Available from: <https://doi.org/10.1111/acer.14796>